

---

# Comparison of $^{18}\text{F}$ -FDG and $^{11}\text{C}$ -Methionine for PET-Guided Stereotactic Brain Biopsy of Gliomas

Benoit Pirotte, MD<sup>1</sup>; Serge Goldman, MD, PhD<sup>2</sup>; Nicolas Massager, MD<sup>1</sup>; Philippe David, MD<sup>3</sup>; David Wikler, MS<sup>1</sup>; Arlette Vandesteene, MD, PhD<sup>4</sup>; Isabelle Salmon, MD, PhD<sup>5</sup>; Jacques Brotchi, MD, PhD<sup>1</sup>; and Marc Levivier, MD, PhD<sup>1</sup>

<sup>1</sup>Department of Neurosurgery, Erasme Hospital, Université Libre de Bruxelles, Brussels, Belgium; <sup>2</sup>PET/Biomedical Cyclotron Unit, Erasme Hospital, Université Libre de Bruxelles, Brussels, Belgium; <sup>3</sup>Department of Neuroradiology, Erasme Hospital, Université Libre de Bruxelles, Brussels, Belgium; <sup>4</sup>Department of Anesthesiology, Erasme Hospital, Université Libre de Bruxelles, Brussels, Belgium; and <sup>5</sup>Department of Neuropathology, Erasme Hospital, Université Libre de Bruxelles, Brussels, Belgium

---

We compared the contributions of the labeled tracers  $^{11}\text{C}$ -methionine (Met) and  $^{18}\text{F}$ -FDG for PET-guided stereotactic biopsy of brain gliomas. **Methods:** In 32 patients with glioma, stereotactic Met PET and  $^{18}\text{F}$ -FDG PET were integrated in the planning of stereotactic brain biopsy. PET images were analyzed to determine which tracer offered the best information for target definition. The stereotactic coregistration of PET images allowed accurate comparison of the level, distribution, and extent of uptake for both tracers according to tumor location and grade. **Results:** A histologic diagnosis was obtained for all patients. All gliomas had an area of abnormal Met uptake, and 27 showed abnormal  $^{18}\text{F}$ -FDG uptake.  $^{18}\text{F}$ -FDG was used for target selection when its uptake was higher in tumor than in gray matter (14 gliomas). Seven were in the basal ganglia or brain stem. Met was used for target selection when there was no  $^{18}\text{F}$ -FDG uptake or when  $^{18}\text{F}$ -FDG uptake was equivalent to that in the gray matter (18 gliomas). Thirteen were in the cortex. Sixty-one of the 70 stereotactic trajectories obtained from the 32 patients were based on PET-defined targets and had an area of abnormal Met uptake. These 61 Met-positive trajectories always yielded a diagnosis of tumor. All nondiagnostic trajectories ( $n = 9$ ) were obtained in areas with no increased uptake of Met. In all patients with increased uptake of both tracers, the focus of highest Met uptake corresponded to the focus of highest  $^{18}\text{F}$ -FDG uptake. However, the extent of uptake of both tracers was variable. **Conclusion:** Distributions of highest Met and  $^{18}\text{F}$ -FDG uptake are similar in brain gliomas. Because Met provides a more sensitive signal, it is the molecule of choice for single-tracer PET-guided neurosurgical procedures in gliomas.

**Key Words:** stereotactic biopsy; PET;  $^{18}\text{F}$ -FDG;  $^{11}\text{C}$ -methionine; glioma

**J Nucl Med 2004; 45:1293–1298**

**B**ecause brain tumors are histologically heterogeneous, CT- or MRI-guided stereotactic brain biopsy does not always yield a valid diagnosis or grading (1–5). PET provides useful, independent, and complementary metabolic information on brain tumors (5–8). We previously described a technique allowing the routine integration of PET data in the planning of stereotactic brain biopsy (9–12). We originally used  $^{18}\text{F}$ -FDG as the unique radiotracer because of the large core of information on the use of this tracer in neurooncology. The selection of targets on stereotactic PET images with  $^{18}\text{F}$ -FDG allows biopsies to be directed accurately toward the hypermetabolic foci of brain tumors (9,10). We have shown that  $^{18}\text{F}$ -FDG PET-guided stereotactic brain biopsy increases the diagnostic yield and accuracy of the technique (9–11,13).

Still, experience with  $^{18}\text{F}$ -FDG PET-guided biopsy has shown some limitations. Indeed, targeting may be difficult when there is no or minor  $^{18}\text{F}$ -FDG uptake, such as in low-grade tumors (14). Also, when a hypermetabolic lesion is near the cortical or subcortical gray matter, tumor  $^{18}\text{F}$ -FDG uptake and normal  $^{18}\text{F}$ -FDG uptake are difficult to differentiate (14–15). Therefore, we tested  $^{11}\text{C}$ -methionine (Met) as an alternative tracer for stereotactic PET guidance. The use of Met, a marker of amino acid uptake and protein synthesis, has also been validated in neurooncology (14,16–22). This PET tracer has several advantages: It is considered efficient and more suitable than  $^{18}\text{F}$ -FDG for delineating areas of tumor tissue (18,19,23,24); its uptake has been shown to be increased in low-grade glial tumors (15,17,18,24,25); its uptake is low in gray matter; and its biologic behavior in neoplastic tissues shows that its accumulation represents active transport of amino acids.

As a first step toward the use of PET with Met (Met PET) in stereotactic conditions, we previously used combined  $^{18}\text{F}$ -FDG and Met PET guidance for stereotactic brain biopsy (26). The aim of the present study was to compare the

---

Received Nov. 29, 2003; revision accepted Feb. 11, 2004.  
For correspondence or reprints contact: Benoit Pirotte, MD, Department of Neurosurgery, Erasme Hospital, Université Libre de Bruxelles, 808, Route de Lennik, 1070 Brussels, Belgium.  
E-mail: bpirotte@ulb.ac.be

distribution, extent, and relative contributions of Met and  $^{18}\text{F}$ -FDG in a series of glioma patients who underwent PET-guided stereotactic brain biopsy with both tracers.

## MATERIALS AND METHODS

### Patient Selection

Since June 1991, we have routinely performed PET-guided stereotactic brain biopsy on patients suspected, on the basis of a preoperative neuroimaging work-up, of having a nonresectable brain tumor. Our current series comprised more than 250 patients. Between July 1992 and June 1997, 45 consecutive patients underwent biopsy guided by combined  $^{18}\text{F}$ -FDG PET and Met PET performed under stereotactic conditions. The double-tracer procedure was proposed for those patients because they presented with a tumor considered unresectable and located in the cortical or subcortical gray matter (including the basal ganglia and the brain stem). Thirty-two of the patients had a diagnosis of glioma. They were 20 men and 12 women whose ages ranged from 2 to 85 y (mean, 52.6 y). All patients were previously untreated.

### Stereotactic PET Data Acquisition

For data acquisition, the technique of combined stereotactic PET with Met and  $^{18}\text{F}$ -FDG was adapted from our previous experience with  $^{18}\text{F}$ -FDG PET-guided stereotactic brain biopsy (9–11). Placement of the stereotactic frame; data acquisition, including stereotactic PET with Met and  $^{18}\text{F}$ -FDG, and CT or MRI; surgical planning; and biopsy were performed on the same day. All patients gave informed consent, and the procedure met the ethical guidelines of our institution.

After placement of the CT- and MRI-compatible base ring (Fischer ZD-Neurosurgical Localizing Unit; Howmedica Leibinger), stereotactic CT or MRI without and with intravenous contrast enhancement was performed. For stereotactic PET, a clamp specifically designed to secure the head ring to the Siemens couch (Howmedica Leibinger) was used. To create a fiducial reference system compatible with PET, we used the commercial MRI localizers with minor modifications as previously described (9–10). After the transmission scan, the patient first received an intravenous injection of 370–555 MBq of Met. Met PET images used for stereotactic calculation were acquired between 20 and 40 min after injection of the tracer. Eighty minutes after Met injection, the patient was injected with 74–185 MBq of  $^{18}\text{F}$ -FDG (specific activity > 74 Bq/ $\mu\text{mol}$ ).  $^{18}\text{F}$ -FDG PET images used for stereotactic calculation were acquired between 40 and 60 min later. The PET camera (933/08/12 tomograph; CTI/Siemens) allowed simultaneous 2-dimensional acquisition of 15 slices about 6.5 mm thick, with a resolution of about 5 mm in full width at half maximum.

### Analysis of Stereotactic PET Images and Target Definition

The surgical planning began with analysis of the PET images. Because this series represented an evaluation of Met PET, we always started with an independent analysis of  $^{18}\text{F}$ -FDG PET images based on our previous experience (9–11). Met PET images were analyzed afterward. Areas of abnormal metabolism used for target selection were either zones of  $^{18}\text{F}$ -FDG or Met uptake that were higher than the surrounding normal-appearing brain tissue or foci of relatively increased  $^{18}\text{F}$ -FDG or Met uptake in a hypometabolic lesion.  $^{18}\text{F}$ -FDG was used for target selection when its uptake in the tumor was higher than, or distinguishable from, the gray

matter. To be considered distinguishable from the gray matter,  $^{18}\text{F}$ -FDG uptake needed to be outside normally located or displaced gray matter. This was evaluated on coregistered PET and MR images. Met was used for target selection when there was no  $^{18}\text{F}$ -FDG uptake or when  $^{18}\text{F}$ -FDG uptake was attributable to metabolic activity in gray matter. If the PET images revealed areas of abnormally increased tracer uptake within the area of the lesion, the plane that best displayed the abnormal  $^{18}\text{F}$ -FDG or Met uptake was selected. On visual inspection, the surgeon interactively pointed at a pixel in the center of this zone, and its calculated coordinates set a target for biopsy. Because, in all cases, the biopsy was planned to establish a histologic diagnosis and not to define the extension of the lesion, all PET-defined targets were maintained within the boundaries of the lesion on CT or MRI. When a target was selected on  $^{18}\text{F}$ -FDG PET, it was then projected onto the corresponding Met PET slice to analyze and compare the local uptake of both tracers. The targets were also projected onto the corresponding stereotactic CT or MRI slice to control the reliability and safety of the target selection and trajectory.

Whenever possible, 2 targets sampling different metabolic areas of the tumor were selected for biopsy. When the area of highest  $^{18}\text{F}$ -FDG uptake was smaller than the limits of the lesion visualized on the corresponding slice of Met PET, another target was selected on the Met PET image, outside the area of increased  $^{18}\text{F}$ -FDG uptake. In patients with no obvious abnormal  $^{18}\text{F}$ -FDG or Met uptake that could be used to select a target for biopsy, surgery was planned using CT or MRI data only.

### Data Analysis

In all patients, serial stereotactic biopsies were performed along each trajectory, following the technique described by Kelly et al. (27). For all biopsy specimens, smear preparation and formalin-fixed samples were analyzed after appropriate staining (9–11,28,29). Gliomas were classified using a 3-tier system: low-grade glioma (LGG), including astrocytoma, oligodendroglioma, giant cell astrocytoma, and gangliocytoma; anaplastic astrocytoma (AA); and glioblastoma (GB).

For each patient, a histologic diagnosis was established. Then, the pathologic description obtained for each biopsy trajectory was recorded separately, regardless of the patient's final diagnosis. If nontumor samples made of gliotic, inflammatory, or necrotic tissue were found, they were classified as nondiagnostic trajectories.

In order to evaluate the role of Met PET in target selection, we retrospectively classified biopsy trajectories in 3 groups, according

**TABLE 1**  
Target Definition in 32 PET-Guided Stereotactic Biopsy Procedures

Diagnosis	$^{18}\text{F}$ -FDG-defined target (FDGt > FDGgm)	Met-defined target	
		FDGt = FDGgm	FDGt < FDGgm
GB	7	3	—
AA	6	5	1
LGG	1	5	4
Total	14	13	5

FDGt =  $^{18}\text{F}$ -FDG uptake in tumor; FDGgm =  $^{18}\text{F}$ -FDG uptake in surrounding gray matter.

**TABLE 2**  
Target Definition in 20 Gliomas in Cortex

Diagnosis	<sup>18</sup> F-FDG–defined target (FDGt > FDGgm)	Met-defined target	
		FDGt = FDGgm	FDGt < FDGgm
GB	4	2	—
AA	2	5	1*
LGG	1	2	3*
Total	7	9	4*

\*Not enhanced after contrast on CT/MR.

FDGt = <sup>18</sup>F-FDG uptake in tumor; FDGgm = <sup>18</sup>F-FDG uptake in surrounding gray matter.

to their metabolic characteristics: <sup>18</sup>F-FDG PET–guided trajectory, Met PET–guided trajectory, and CT/MRI-guided trajectory. For that purpose and because we found that all areas of increased <sup>18</sup>F-FDG uptake were within areas of increased Met uptake, we first looked at whether areas of increased Met uptake were present [Met(+)] or absent [Met(-)]. In Met(+) trajectories, we further looked at whether <sup>18</sup>F-FDG PET was used for the target selection. Indeed, as already described, <sup>18</sup>F-FDG PET images were used first for target selection (<sup>18</sup>F-FDG PET–guided trajectory). When <sup>18</sup>F-FDG PET did not provide information considered valid for target selection, Met PET was used (Met PET–guided trajectory). In Met(-) trajectories, target selection was based on CT or MRI only (CT/MRI-guided trajectory).

## RESULTS

A total of 70 stereotactic biopsy trajectories were performed on the 32 patients (2.2 trajectories per patient). A histologic diagnosis was obtained for all patients. The diagnoses included 10 GBs, 12 AAs, and 10 LGGs (6 astrocytomas, 2 oligodendrogliomas, 1 giant cell astrocytoma, and 1 gangliocytoma).

In all cases, a PET-defined target could be set using either the <sup>18</sup>F-FDG data or the Met data (Table 1). All gliomas had

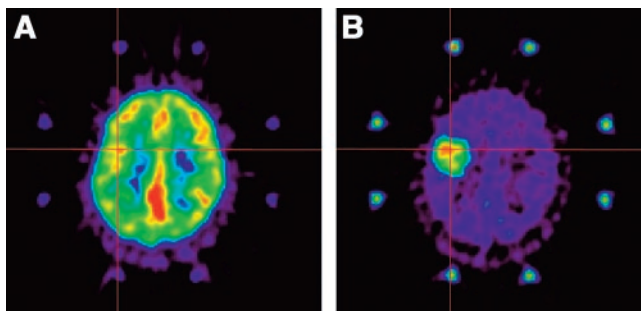


**FIGURE 1.** PET performed with <sup>18</sup>F-FDG (A) and Met (B) on a 32-y-old man with an AA in the left frontorolandic cortical area. Uptake of <sup>18</sup>F-FDG in tumor was equivalent to that in cortical gray matter. Uptake of Met was higher in tumor than in cortex, allowing definition of a target for biopsy. When PET images obtained with the 2 tracers were coregistered, the focus of highest Met uptake corresponded to the unique focus of <sup>18</sup>F-FDG uptake within the tumor (crosses).

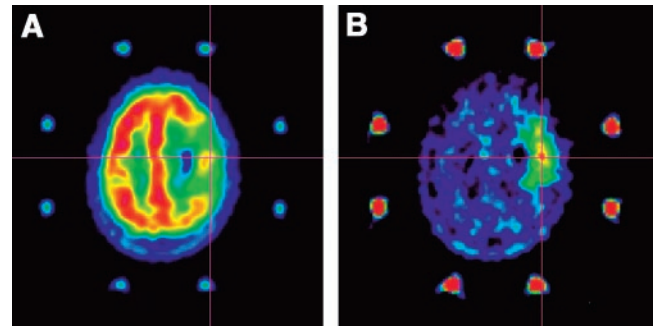


**FIGURE 2.** PET performed with <sup>18</sup>F-FDG (A) and Met (B) on a 62-y-old woman with a GB in the right prerolandic cortical area. Uptake of <sup>18</sup>F-FDG was reduced in the tumor area except for 1 spot of uptake equivalent to that in the surrounding gray matter. Uptake of Met was higher in tumor than in cortex, allowing definition of a target for biopsy. When PET images obtained with the 2 tracers were coregistered, the highest focus of Met uptake corresponded to the hot spot of <sup>18</sup>F-FDG (crosses).

an area of abnormal Met uptake, and 27 showed abnormal <sup>18</sup>F-FDG uptake. When <sup>18</sup>F-FDG uptake was higher in tumor than in gray matter ( $n = 14$ ), that tracer was used for target selection. This occurred in 7 GBs, 6 AAs, and 1 LGG. Met was the tracer used to define a biopsy target for the other 18 tumors (56%). These corresponded to 9 high-grade tumors and 9 LGGs.

Twenty of the 32 gliomas involved the cortical area, and Met was used for target selection for 13 of them (65%) (Table 2; Figs. 1 and 2). The 13 cortical gliomas targeted on Met PET included 4 that were not enhanced on CT or MRI (3 LGGs and 1 AA). The other 12 gliomas involved either the basal ganglia ( $n = 10$ ) or the brain stem ( $n = 2$ ) (Table 3; Figs. 3 and 4). In 7 of these 12 gliomas (58%), <sup>18</sup>F-FDG was used for target selection. However, in 1 GB (patient 10), a second trajectory was performed in an area of high Met uptake outside the limits of high <sup>18</sup>F-FDG uptake and yielded similar tumor tissue.

Table 4 analyses the diagnostic yield of the 70 stereotactic trajectories performed on the 32 patients according to

**TABLE 3**  
Target Definition in 12 Gliomas in Basal Ganglia or Brain Stem

Diagnosis	<sup>18</sup> F-FDG–defined target (FDGt > FDGgm)	Met-defined target	
		FDGt = FDGgm	FDGt < FDGgm
GB	3	1	—
AA	4	—	—
LGA	—	3*	1*
Total	7	4*	1*

\*One tumor of the group was not enhanced after contrast on CT/MR.

FDGt = <sup>18</sup>F-FDG uptake in tumor; FDGgm = <sup>18</sup>F-FDG uptake in surrounding gray matter.

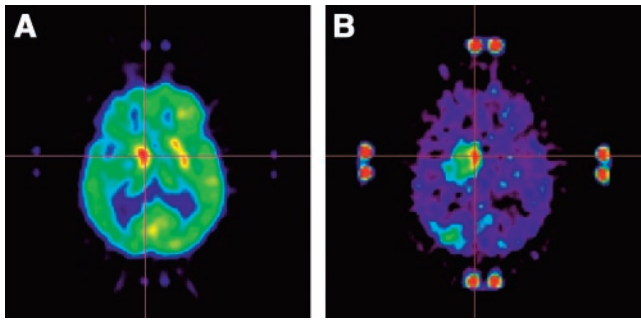


**FIGURE 3.** PET performed with  $^{18}\text{F}$ -FDG (A) and Met (B) on a 74-y-old man with a GB in the right basal ganglia. Uptake of  $^{18}\text{F}$ -FDG was higher in tumor than in surrounding gray matter and allowed definition of a target for biopsy. Uptake of Met was also higher in tumor than in surrounding gray matter, and zones of highest uptake of both tracers corresponded on coregistered images (crosses).

their Met uptake. Sixty-one trajectories corresponded to an area of increased Met uptake. The other 9 trajectories showed no abnormal Met uptake, and biopsy was based on CT- or MRI-defined targets. All 61 Met(+) trajectories yielded tumor tissue, whereas the 9 Met(-) trajectories yielded nontumor tissue and were nondiagnostic. In 22 trajectories,  $^{18}\text{F}$ -FDG uptake was higher in the tumor than in the gray matter. This group included 11 GB, 10 AA, and 1 LGG samples. The targets used to define these trajectories were all CT or MRI enhanced. Thirteen (59%) were in the basal ganglia or the brain stem. In 22 other trajectories, tumor  $^{18}\text{F}$ -FDG uptake was equivalent to that of the gray matter. This group included 7 GB, 9 AA, and 6 LGG samples. Sixteen targets corresponded to enhanced areas on CT or MRI and 6 to unenhanced areas. Finally, 17 trajectories had very low or no tumor  $^{18}\text{F}$ -FDG uptake and were guided on Met PET. They included 3 AA and 15 LGG samples. All hypodense or hyposignal targets on CT or MRI were in this group. Thus, Met was used efficiently to define the biopsy target for 39 of the 61 trajectories (64%).

All Met(-) nondiagnostic trajectories occurred in patients for whom the diagnosis was obtained from another trajectory that presented increased Met uptake. These diagnoses included 2 GBs, 3 AAs, and 4 LGGs. Among them, 5

were targets with no contrast enhancement on MRI. One showed discrete but significant enhancement on MRI.

This study also allowed us to correlate the  $^{18}\text{F}$ -FDG- and Met PET images stereotactically and to compare the tumor level, extent, and distribution of the 2 tracers. Of the 14 gliomas in which uptake of both tracers was higher than in surrounding gray matter, Met uptake was more extended than  $^{18}\text{F}$ -FDG uptake in 10 (Fig. 4) and equally extended in 4. In all cases, the focus of highest Met uptake corresponded to the focus of highest  $^{18}\text{F}$ -FDG uptake (Figs. 3 and 4). When tumor  $^{18}\text{F}$ -FDG uptake was equivalent to  $^{18}\text{F}$ -FDG uptake in the surrounding gray matter (13 gliomas), the projection of the highest Met uptake on  $^{18}\text{F}$ -FDG PET images corresponded to an individualized focus of highest  $^{18}\text{F}$ -FDG uptake within the gray matter in 5 of 8 high-grade gliomas. Still, on the  $^{18}\text{F}$ -FDG scans, these foci were not differentiated from the rest of the gray matter (Figs. 1 and 2). For the 5 LGGs in which  $^{18}\text{F}$ -FDG uptake was equivalent to that in surrounding gray matter, the areas of highest uptake of Met and  $^{18}\text{F}$ -FDG never matched.

## DISCUSSION

Brain tumors, especially gliomas, are characterized by regional variations of histologic malignancy (24,30) that cannot be distinguished on conventional anatomic imaging such as MRI even with contrast injection (31). Therefore CT- or MRI-guided stereotactic brain biopsy does not always yield valid diagnosis or grading, since target selection may lead to a significant sampling error and secondary understaging (1-5).

PET provides independent and complementary metabolic information on brain tumors (5-8). The literature has collected numerous data on PET of brain tumors, mainly with the tracer  $^{18}\text{F}$ -FDG. When combined with anatomic imaging techniques,  $^{18}\text{F}$ -FDG PET can provide information on tumor grading (11,32,33), response to therapy (34), and prognosis (35,36). In particular, early clinical studies have demonstrated that the glycolytic rate of brain tumors, as assessed by  $^{18}\text{F}$ -FDG uptake, is a more accurate reflection of tumor grade than is contrast enhancement (31).

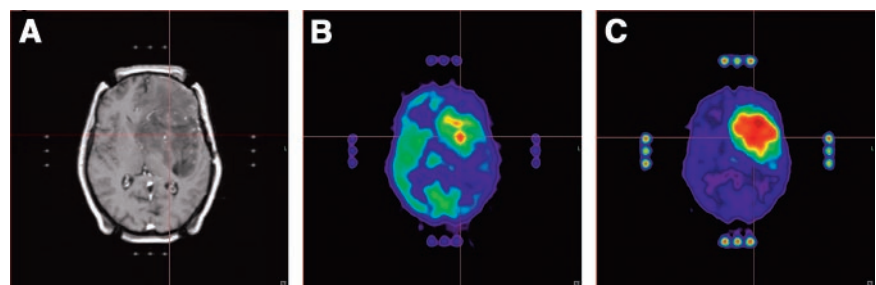


**FIGURE 4.** MRI (A) and PET performed with  $^{18}\text{F}$ -FDG (B) and Met (C) on a 57-y-old woman with an infiltrating AA in the left basal ganglia and subcortical frontal region. Uptake of  $^{18}\text{F}$ -FDG was higher in tumor than in surrounding gray matter and allowed definition of a target for biopsy. Uptake of Met was also higher in tumor than in surrounding gray matter. Coregistration of PET images showed that Met uptake was more extended than  $^{18}\text{F}$ -FDG uptake but that zones of highest uptake corresponded (crosses).

**TABLE 4**  
Diagnostic Yield and  $^{18}\text{F}$ -FDG/ $^{11}\text{C}$ -Methionine Uptake of 70 Biopsy Trajectories

Diagnosis	Met(+) trajectories			Met(-) trajectories (FDGt < FDGgm)
	FDGt > FDGgm	FDGt = FDGgm	FDGt < FDGgm	
GB	11	7	—	—
AA	10	9	2	—
LGG	1	6	15	—
Nondiagnostic	—	—	—	9
Total	22	22	17	9

FDGt =  $^{18}\text{F}$ -FDG uptake in tumor; FDGgm =  $^{18}\text{F}$ -FDG uptake in surrounding gray matter.

To take advantage of these metabolic data in the management of brain tumors, we previously developed a technique allowing the routine integration of PET data in the planning of stereotactic brain biopsy (9,10). We originally used  $^{18}\text{F}$ -FDG because it was the most widely used radiotracer for brain tumors (24). The selection of targets on stereotactic  $^{18}\text{F}$ -FDG PET-generated images allows biopsies to accurately be directed toward the abnormal metabolic foci of brain tumors (9,10). We have shown that  $^{18}\text{F}$ -FDG PET-guided stereotactic brain biopsy increases the diagnostic yield and accuracy of the technique (11–13). Moreover, PET-guided stereotactic brain biopsy has allowed accurate correlation of metabolism and histology and confirmation of the correlation between PET tracer uptake and tumor grade (21). Indeed, with this method we have found a significant relationship between  $^{18}\text{F}$ -FDG uptake, as well as Met uptake, and the presence of anaplasia (29,30).

Our results confirm our preliminary data showing that Met may be a good alternative to  $^{18}\text{F}$ -FDG for target selection in PET-guided stereotactic brain biopsy (26).

With Met PET guidance, a histologic diagnosis was obtained for all patients. The 9 nondiagnostic samples were exclusively from trajectories defined on CT or MRI in areas with no Met uptake. Because CT or MRI findings were abnormal in those areas, one cannot rule out the possibility that biopsy guidance limited to CT/MRI data in those 9 patients would have led to the final diagnosis. This high diagnostic value of Met PET is also illustrated by the fact that, in this series of patients, all gliomas presented as an area of increased Met uptake.

Our experience with both tracers, acquired and compared under stereotactic conditions, shows that, in 18 of the 32 gliomas, all of which were in gray matter, Met was the only tracer that could safely be used for target selection. This was the case for AAs and GBs in which tumor  $^{18}\text{F}$ -FDG uptake and normal  $^{18}\text{F}$ -FDG uptake were difficult to differentiate, as well as for LGGs in which there was no  $^{18}\text{F}$ -FDG uptake. Indeed, in 9 LGGs, the highest focus of Met uptake was used for target definition. One could argue that Met uptake in LGG is not a constant finding (18,35). However, the chance of finding abnormally increased uptake of radiotracer remains higher with Met than with  $^{18}\text{F}$ -FDG (32,33,37).

When located in the cortex, most high-grade gliomas (14/20) limited the ability of  $^{18}\text{F}$ -FDG PET to define a target. Met is therefore superior to  $^{18}\text{F}$ -FDG for target selection in enhanced or unenhanced gliomas in the cortex. When the glioma was in subcortical gray matter,  $^{18}\text{F}$ -FDG was more frequently useful for target selection: In 7 of 12 cases  $^{18}\text{F}$ -FDG was useful, whereas in the other 5 only Met showed abnormal uptake. All stereotactic biopsies performed on brain stem gliomas yielded a diagnosis of tumor, as anticipated by a high uptake of Met. This further confirms that the integration of stereotactic PET, especially with Met, should allow an increase in diagnostic yield while reducing the number of trajectories in highly functional brain areas (13).

Because Met uptake was increased in all gliomas, whatever the grade, one could argue that Met PET was not discriminating enough to direct the biopsy to the most malignant area of the tumor, as allowed by  $^{18}\text{F}$ -FDG PET (11). With stereotactic coregistration, however, we found that the area of highest Met uptake and the area of highest  $^{18}\text{F}$ -FDG uptake usually corresponded. This observation confirms the findings of our previous study of Met and  $^{18}\text{F}$ -FDG uptake in biopsy samples. That study demonstrated a significant correlation between the uptake of both tracers and the degree of anaplasia (33).

Because Met provides better information than  $^{18}\text{F}$ -FDG on tumor extent, Met has already gained a place, in combination with MRI, in the neurosurgical strategies aimed at delineating the entire tumor volume, either for resection under neuronavigation or for radiosurgery (38–40). In this series, Met has also appeared suitable for “within-tumor” biopsy planning. Further tests should be conducted with  $^{18}\text{F}$ -labeled amino acids to make the method accessible in centers not able to produce tracers in-house (23).

## CONCLUSION

The results of the current retrospective analysis confirm that Met can be used accurately as a radiotracer for routine image-guided neurosurgery of brain gliomas. Compared with  $^{18}\text{F}$ -FDG, Met offers an equivalent possibility of target selection in areas of highest metabolic activity. The higher sensitivity of Met makes it the best

choice for single-tracer PET-guided stereotactic brain biopsy.

## REFERENCES

1. Black PM. Brain tumors (second of two parts). *N Engl J Med*. 1991;324:1555–1564.
2. Chandrasoma PT, Smith MM, Apuzzo MLJ. Stereotactic biopsy in the diagnosis of brain masses: comparison of results of biopsy and resected surgical specimen. *Neurosurgery*. 1989;24:160–165.
3. Choksey MS, Valentine A, Shawdon H, Freer CER, Lindsay KD. Computed tomography in the diagnosis of malignant brain tumours: do all patients require biopsy? *J Neurol Neurosurg Psychiatry*. 1989;52:821–825.
4. Feiden W, Steude U, Bise K, Gündisch O. Accuracy of stereotactic brain tumor biopsy: comparison of the histologic findings in biopsy cylinders and resected tumor tissue. *Neurosurg Rev*. 1991;14:51–56.
5. Glantz MJ, Burger PC, Herndon JE II, et al. Influence of the type of surgery on the histological diagnosis in patients with anaplastic gliomas. *Neurology*. 1991;41:1741–1744.
6. Alavi J, Alavi A, Chawluk J, et al. Positron emission tomography in patients with glioma: a predictor of prognosis. *Cancer*. 1988;62:1074–1078.
7. Di Chiro G. Positron emission tomography using [<sup>18</sup>F] fluorodeoxyglucose in brain tumors: a powerful diagnostic and prognostic tool. *Invest Radiol*. 1986;22:360–371.
8. Patronas NJ, Di-Chiro G, Kufta C, et al. Prediction of survival in glioma patients by means of positron emission tomography. *J Neurosurg*. 1985;62:816–822.
9. Pirotte B, Goldman S, Brucher JM, et al. PET in stereotactic conditions increases the diagnostic yield of brain biopsy. *Stereotact Funct Neurosurg*. 1994;63:144–149.
10. Pirotte B, Goldman S, Bidaut L, et al. Use of positron emission tomography (PET) in stereotactic conditions for brain biopsy. *Acta Neurochir*. 1995;134:79–82.
11. Levivier M, Goldman S, Pirotte B, et al. Diagnostic yield of stereotactic brain biopsy guided by positron emission tomography with [<sup>18</sup>F]fluorodeoxyglucose. *J Neurosurg*. 1995;82:445–452.
12. Pirotte B, Goldman S, Salzberg S, et al. Combined positron emission tomography and magnetic resonance imaging for the planning of stereotactic brain biopsies in children: experience in 9 cases. *Pediatr Neurosurg*. 2003;38:146–155.
13. Massager N, David P, Goldman S, et al. Combined MRI—and PET—guided stereotactic biopsy in brainstem mass lesions: diagnostic yield in a series of 30 patients. *J Neurosurg*. 2000;93:951–957.
14. Chung JK, Kim YK, Kim SK, et al. Usefulness of <sup>11</sup>C-methionine PET in the evaluation of brain lesions that are hypo- or isometabolic on <sup>18</sup>F-FDG-PET. *Eur J Nucl Med Mol Imaging*. 2002;29:176–182.
15. Delbeke D, Meyerowitz C, Lapidus RL, et al. Optimal cutoff levels of F-18 fluorodeoxyglucose uptake in the differentiation of low-grade from high-grade brain tumors with PET. *Radiology*. 1995;195:47–52.
16. Bergstrom M, Ericson K, Hagenfeldt L, et al. PET study of methionine accumulation in glioma and normal brain tissue: competition with branched chain amino acids. *J Comput Assist Tomogr*. 1987;11:208–213.
17. Derlon JM, Bourdet C, Bustany P, et al. [<sup>11</sup>C]L-methionine uptake in gliomas. *Neurosurgery*. 1989;25:720–728.
18. Derlon JM, Petit-Taboué M-C, Chapon F, et al. The *in vivo* metabolic pattern of low-grade brain gliomas: a positron emission tomographic study using <sup>18</sup>F-fluorodeoxyglucose and <sup>11</sup>C-L-methylmethionine. *Neurosurgery*. 1997;40:276–288.
19. Ericson K, Lilja A, Bergstrom M, et al. Positron emission tomography with (<sup>11</sup>C)methyl-L-methionine, [<sup>11</sup>C]D-glucose, and [<sup>68</sup>Ga]EDTA in supratentorial tumors. *J Comput Assist Tomogr*. 1985;9:683–689.
20. Mineura K, Sasajima T, Kowada M, et al. Innovative approach in the diagnosis of gliomatosis cerebri using carbon-11-L-methionine positron emission tomography. *J Nucl Med*. 1991;32:726–728.
21. Mosskin M, von Holst H, Bergström M, et al. Positron emission tomography with <sup>11</sup>C-methionine and computed tomography of intracranial tumours compared with histopathologic examination of multiple biopsies. *Acta Radiol*. 1987;28:673–681.
22. Ogawa T, Shishido F, Kanno I, et al. Cerebral glioma: evaluation with methionine PET. *Radiology*. 1993;186:45–53.
23. Wienhard K, Herholz K, Coenen HH, et al. Increased amino acid transport into brain tumors measured by PET of L-(2-<sup>18</sup>F)fluorotyrosine. *J Nucl Med*. 1991;32:1338–1346.
24. Wong TZ, Van der Westhuizen GJ, Coleman RE. Positron emission tomography imaging of brain tumors. *Neuroimaging Clin North Am*. 2002;12:615–626.
25. Kaschten B, Stevenaert A, Sadzot B, et al. Preoperative evaluation of 54 gliomas by PET with fluorine-18-fluorodeoxyglucose and/or carbon-11-methionine. *J Nucl Med*. 1998;39:778–785.
26. Pirotte B, Goldman S, David P, et al. Stereotactic brain biopsy guided by positron emission tomography with [<sup>18</sup>F]fluorodeoxyglucose and [<sup>11</sup>C]methionine. *Acta Neurochir*. 1997;68:133–138.
27. Kelly PJ, Daumas-Duport C, Kispert DB, et al. Imaging-based stereotactic serial biopsies in untreated intracranial glial neoplasms. *J Neurosurg*. 1987;66:865–874.
28. Kleihues P, Burger PC, Scheithauer BW. The new WHO classification of brain tumors. *Brain Pathol*. 1993;3:255–268.
29. Salmon I, Levivier M, Camby I, et al. Assessment of nuclear size, nuclear DNA content and proliferation index in stereotactic biopsies from brain tumours. *Neuropathol Appl Neurobiol*. 1993;19:507–518.
30. Paulus W, Peiffer J. Intratumoral histologic heterogeneity of gliomas: a quantitative study. *Cancer*. 1989;64:442–447.
31. Patronas NJ, Brooks RA, DeLaPaz RL, et al. Glycolytic rate (PET) and contrast enhancement (CT) in human cerebral gliomas. *AJNR Am J Neuroradiol*. 1983;4:533–535.
32. Goldman S, Levivier M, Pirotte B, et al. Regional glucose metabolism and histopathology of gliomas: a study based on positron emission tomography-guided stereotactic biopsy. *Cancer*. 1996;78:1098–1106.
33. Goldman S, Levivier M, Pirotte B, et al. Regional methionine and glucose metabolism in gliomas: a comparative study on PET-guided stereotactic biopsy. *J Nucl Med*. 1997;38:1–4.
34. De Witte O, Levivier M, Violon P, et al. Quantitative imaging study of extent of surgical resection and prognosis of malignant astrocytomas. *Neurosurgery*. 1998;43:398–399.
35. De Witte O, Levivier M, Violon P, et al. Prognostic value of positron emission tomography with [<sup>18</sup>F]fluoro-2-deoxy-D-glucose in the low-grade glioma. *Neurosurgery*. 1996;39:470–476.
36. De Witte O, Lefranc F, Levivier M, et al. FDG-PET as a prognostic factor in high-grade astrocytoma. *J Neurooncol*. 2000;49:157–163.
37. De Witte O, Goldberg I, Wikler D, et al. Positron emission tomography with injection of methionine as a prognostic factor in glioma. *J Neurosurg*. 2001;95:746–750.
38. Levivier M, Wikler D, Goldman S, et al. Positron emission tomography in stereotactic conditions as a functional imaging technique for neurosurgical guidance. In: Alexander EB III, Maciunas RM, eds. *Advanced Neurosurgical Navigation*. New York, NY: Thieme Medical Publishers, Inc.; 1999:85–99.
39. Levivier M, Wikler D, Massager N, et al. The integration of metabolic imaging in stereotactic procedures including radiosurgery: a review. *J Neurosurg*. 2002;97:542–550.
40. Levivier M, Massager N, Wikler D, et al. Use of stereotactic PET images in dosimetry planning of radiosurgery for brain tumors: clinical experience and proposed classification. *J Nucl Med*. 2004;45:1146–1154.